




BACH1 promotes clear cell renal cell carcinoma progression by upregulating oxidative stress-related tumorigenicity

Kenshiro Takemoto^{1,2}  | Kohei Kobatake¹  | Kento Miura² | Takafumi Fukushima¹ | Takashi Babasaki¹ | Shunsuke Miyamoto¹ | Yohei Sekino¹ | Hiroyuki Kitano¹ | Keisuke Goto¹ | Kenichiro Ikeda¹ | Keisuke Hieda¹ | Tetsutaro Hayashi¹ | Nobuyuki Hinata¹  | Osamu Kaminuma²

¹Department of Urology, Graduate School of Biomedical and Health Sciences, Hiroshima University, Hiroshima, Japan

²Department of Disease Models, Research Institute for Radiation Biology and Medicine, Hiroshima University, Hiroshima, Japan

Correspondence

Kohei Kobatake, Department of Urology, Graduate School of Biomedical and Health Sciences, Hiroshima University, 1-2-3 Kasumi, Minamiku, Hiroshima 734-8551, Japan.

Email: kkobatake@hiroshima-u.ac.jp

Funding information

JSPS KAKENHI, Grant/Award Number: 21K09426; Joint Research Grant from the Research Center for Radiation Disaster Medical Science

Abstract

The carcinogenesis and progression of renal cell carcinoma (RCC), a heterogeneous cancer derived from renal tubular epithelial cells, is closely related to oxidative stress responses (OSRs). Oxidative stress responses participate in various biological processes related to the metabolism and metastatic potential of cancer such as inflammation, epithelial–mesenchymal transition (EMT), and angiogenesis. In this study, we investigated the role of broad complex–tramtrack–bric-a-brac and cap 'n' collar homology 1 (BACH1), a key transcription factor for OSRs, in clear cell RCC (ccRCC) development and prognosis. The poor prognosis and elevation of serum inflammation markers in nephrectomized ccRCC patients were correlated with the intratumor expression of BACH1 accompanied by a downregulation of heme oxygenase-1. BACH1 contributes to the invasion and migration abilities of RCC cell lines without affecting their proliferation in vitro. In contrast, BACH1 contributes to tumor progression in vivo, in relation to OSRs with the activation of EMT-related pathways. BACH1 involvement in other OSR-linked pathways, including inflammatory responses, angiogenesis, and mTOR signaling, was further revealed by RNA sequencing analysis of BACH1-knockdown cells. In conclusion, the crucial role of BACH1 in the pathogenesis and poor prognosis of ccRCC through the promotion of OSRs is suggested.

KEYWORDS

biomarker, oxidative stress response, progression, renal cell carcinoma, tumorigenic activity

Abbreviations: BACH1, broad complex–tramtrack–bric-a-brac and cap 'n' collar homology 1; ccRCC, clear cell renal cell carcinoma; CRP, C-reactive protein; Ct, cycle threshold; EMT, epithelial–mesenchymal transition; FOXA1, forkhead box protein A1; GSSG/GSH, oxidized glutathione/reduced glutathione; GSEA, Gene Set Enrichment Analysis; HO-1, heme oxygenase-1; NLR, neutrophil-to-lymphocyte ratio; OSR, oxidative stress response; qRT-PCR, quantitative RT-PCR; RB, retinoblastoma protein; RCC, renal cell carcinoma; ROS, reactive oxygen species; RRID, Research Resource Identifier; TCGA, The Cancer Genome Atlas; TKI, tyrosine kinase inhibitor; VEGF, vascular endothelial growth factor.

This is an open access article under the terms of the [Creative Commons Attribution-NonCommercial](https://creativecommons.org/licenses/by-nc/4.0/) License, which permits use, distribution and reproduction in any medium, provided the original work is properly cited and is not used for commercial purposes.

© 2022 The Authors. *Cancer Science* published by John Wiley & Sons Australia, Ltd on behalf of Japanese Cancer Association.

1 | INTRODUCTION

Renal cell carcinoma, a heterogeneous cancer derived from renal tubular epithelial cells, is the 12th most common solid tumor that develops in more than 400,000 patients per year worldwide.¹ As most RCC cases are found without metastasis, surgical resection has been one of the standard therapies. However, approximately 30% of patients with RCC are diagnosed after metastasis.² Furthermore, patients with metastatic RCC tend to show an abysmal prognosis; therefore, systemic treatments such as molecular-targeted therapy and immunotherapy have been proposed for these patients.³

There are many risk factors for RCC development, including excess bodyweight, hypertension, cigarette smoking, chronic kidney disease, hemodialysis, kidney transplantation, and acquired kidney cystic diseases.⁴⁻⁸ They are mostly related to hypoxia and inflammatory processes, which are recognized to have a strong relationship with each other⁹ and consequently play an important role in cancer progression.¹⁰⁻¹⁴

Hypoxia promotes the generation of ROS, which induce OSRs. Due to their close relationship with various carcinogenic and tumorigenic processes, including inflammation, EMT, and angiogenesis, OSRs are crucially involved in the development of RCC.¹⁵⁻¹⁷

A cap 'n' collar-basic region leucine zipper factor (CNC-bZip) family transcription factor, BACH1 is implicated in OSRs and the resulting upregulation of the metabolism and metastatic potential of cancer.¹⁸ From the identification of BACH1 by Oyake et al.,¹⁹ various biological activities of BACH1, such as regulation of the cell cycle, heme homeostasis, hematopoiesis, and immunity, have been explored.²⁰ BACH1 negatively regulates the inflammation-related gene *HMOX1*, which encodes an antioxidant enzyme, HO-1.¹⁴ Heme oxygenase-1 catalyzes the degradation of heme and is involved in immunomodulatory, cytoprotective, and anti-inflammatory responses.^{21,22} Consequently, BACH1-mediated HO-1 downregulation results in enhanced ROS production.²³ However, the contribution of BACH1 to the development and prognosis of RCC, including the participation of the HO-1-related pathway, has not been investigated.

In this study, we showed that BACH1 expression accompanied by the downregulation of HO-1 is closely related to the poor prognosis of nephrectomized ccRCC patients, in association with its enhanced invasion, migration, and tumor progression activity in RCC cells. Furthermore, by exploring BACH1-mediated and OSR-related biological pathways, it was suggested that the effectiveness of mTOR inhibitors and TKIs in patients with ccRCC could be predicted by examining BACH1 expression.

2 | MATERIALS AND METHODS

2.1 | Subjects

Seventy-seven patients diagnosed with ccRCC who underwent nephrectomy at the Hiroshima University Hospital between April 2002 and December 2012 were included. The pathological

diagnosis was carried out based on the 2016 WHO classification.²⁴ Upon evaluating the patient background and survival prognosis, we obtained relevant clinicopathologic data from the medical records, such as age, sex, pathological TNM stage, tumor grade, and blood biochemical tests. Tumor staging was undertaken according to the 2010 American Joint Committee on Cancer TNM Staging System.²⁵ The study was conducted in accordance with the Declaration of Helsinki and Good Clinical Practice guidelines. All experimental procedures were approved by the Ethics Committee of Hiroshima University Hospital (approval no. E-588-2). All patients provided written informed consent prior to participation.

2.2 | Immunohistochemical staining

Immunohistochemical staining was carried out on tumor sections obtained by nephrectomy, as described previously.²⁶ Briefly, the sections were incubated with anti-BACH1 (1:200; HPA034949; Atlas Antibodies) or anti-HO-1 Ab (1:100; sc-136960; Santa Cruz Biotechnology) for 1 h at room temperature. After washing with PBS containing 0.05% Tween-20, the sections were incubated with anti-rabbit or anti-mouse HRP polymer (Agilent Technologies) for 1 h at room temperature, followed by incubation with 3,3'-diaminobenzidine substrate buffer (Agilent) for 1 min. Upon blinded examination by two independent uropathologists, the staining intensity of the resulting specimens was determined as positive or negative for BACH1 and categorized into four grades (very weak, weak, moderate, or strong) for HO-1.

2.3 | Cell culture

Human RCC cell lines 786-O (RRID: CVCL_1051), Caki-1 (CVCL_0234), and ACHN (CVCL_1067), and a murine RCC cell line RenCa (CVCL_2174) were purchased from the Japanese Collection of Research Bioresources Cell Bank, and maintained at 37°C in a humidified atmosphere containing 5% CO₂ in RPMI-1640 medium (Sigma-Aldrich) supplemented with 10% FBS (Gibco) and 1% penicillin-streptomycin (FUJIFILM Wako Pure Chemical Corporation).

2.4 | Transfection and RNA interference

To knock down BACH1 expression in 786-O, Caki-1, and ACHN cells, we used siRNA-based RNA interference technology. Cells were independently transfected with two different siRNAs against human BACH1 (siBACH1-1 [#s1859] and siBACH1-2 [#s1860]; Stealth RNAi, Thermo Fisher Scientific) or control siRNA (siCtrl; Silencer, Thermo Fisher Scientific) using Lipofectamine RNAiMAX reagent (Thermo Fisher Scientific). The cells were collected 48 and 72 h after RNA and protein extraction, respectively.

2.5 | Lentivirus infection

For ectopic expression of BACH1 in 786-O, Caki-1, and ACHN cells, a human ORF DNA sequence corresponding to the *BACH1* gene was cloned into a lentiviral plasmid, pCDH-MSCV-MCS-EF1-GFP-T2A-Puro (pCDH; [RRID: Addgene_102325](#)). An empty construct of pCDH was used as the negative control. After confirming that the *BACH1* sequence was cloned, the lentiviral constructs were cotransfected with helper plasmids, PMDLg/pRRE, pRSV-Rev ([RRID: Addgene_12253](#)), and pVSV-G ([RRID: Addgene_138479](#)) into Lenti-X 293T cells (Takara) using Lipofectamine 2000 (Thermo Fisher Scientific). All vectors were purchased from Addgene. After 48 h, the lentiviral supernatant was recovered, filtered, concentrated using a Lenti-X concentrator (Takara), and then used to infect the target cells overnight. The resulting infected cells were sorted as GFP-positive cells using a BD FACSAria II flow cytometer (BD Biosciences).

2.6 | CRISPR/Cas9-mediated gene editing

To knock out Bach1 expression in RenCa cells, we used a CRISPR/Cas9-mediated gene editing technique. For this purpose, commercially available Bach1 sgRNA CRISPR/Cas9 All-in-One Lentivector set (Mouse) and CRISPR scrambled sgRNA All-in-One Lentivector (with spCas9) were purchased from Applied Biological Materials. The Lenti-X 293T cells were cotransfected with 1 μ g of the plasmids and third generation packaging mix (Applied Biological Materials) using Lipofectamine 2000 (Thermo Fisher Scientific) transfection reagent. After 48 h, the lentiviral supernatant was recovered, filtered, and then used to infect the RenCa cells overnight. The resulting infected cells were purified by antibiotic selection with puromycin (FUJIFILM Wako Pure Chemical Corporation).

2.7 | Quantitative RT-PCR

Total RNA was isolated using NucleoSpin RNA (Takara), and 500 ng total RNA was reverse-transcribed to cDNA using PrimeScript RT Master Mix (Takara). Quantitative PCR analysis was carried out for the cDNA with SYBR Select Master Mix (Applied Biosystems) using the Step One Plus Real-time PCR System (Applied Biosystems). The Ct values were normalized to the expression of an endogenous housekeeping gene, *HPRT*, and $2^{(-\Delta\Delta Ct)}$ values were calculated for relative quantification. The reactions were carried out in triplicate using the quantitative PCR primers listed in [Table S1](#).

2.8 | Western blot analysis

Western blot analysis was carried out as described previously.²⁷ Briefly, the protein samples were electrophoresed on 5%–20%

precast polyacrylamide gels (SuperSep Ace; FUJIFILM Wako Pure Chemical Corporation) and transferred to nitrocellulose blotting membranes (GE Healthcare Life Science) by electroblotting. The membranes were blocked for 30 min with 5% nonfat dry milk in TBST (10 mM Tris, pH 8.0, 150 mM NaCl, and 0.05% Tween-20) and incubated with primary Abs at 4°C overnight. The primary Abs used in these assays were as follows: anti-human BACH1 (1:2000, #A303-058A; Bethyl Laboratories), anti-mouse Bach1 (1:1000, #66762-1-Ig; Proteintech), anti-HO-1 (1:1000, #sc-136960; Santa Cruz Biotechnology), anti-E-cadherin (1:1000, #14472; Cell Signaling Technology), anti-N-cadherin (1:1000, #13116; Cell Signaling Technology), anti-vimentin (1:1000, #5741; Cell Signaling Technology), anti-p21 (1:1000, #2946; Cell Signaling Technology), anti-p53 (1:1000, #sc-126; Santa Cruz Biotechnology), anti-RB (1:1000, #9309; Cell Signaling Technology), and anti- β -actin (1:5000, #A2228; Sigma-Aldrich).

2.9 | Transwell invasion assay

For the Transwell invasion assay, 24-well cell culture inserts (Corning) and 8.0 μ m pore size ThinCert membranes (Greiner Bio-One) were used. Cells suspended in serum-free medium were seeded in the top chamber after adding serum-containing medium (10% FBS) to the bottom chamber. Twenty-four hours later, the cells that translocated to the bottom surface of the membrane were recovered and counted following Diff-Quick staining.

2.10 | Wound healing assay

We used a wound healing assay to detect cell migration. Cells were seeded in a culture insert (ibidi culture-insert 2 well; ibidi GmbH) at a density of 5.0×10^5 cells/ml. After allowing the cells to adhere overnight, the culture insert was recovered and washed with PBS to remove the nonadherent cells. The cells were then cultured in fresh medium for 10 h. After photographing the plate at the start and end of the culture period, the number of cells that migrated into the wound space was manually counted in three fields per well under light microscopy at 50 \times magnification. Cell migration areas were quantified using ImageJ software (NIH; <https://imagej.nih.gov/ij/>).

2.11 | Cell proliferation assay

Cells (5.0×10^3 /ml) were incubated in a 96-well cell culture plate for 24 h. Cell proliferation was assessed using the Premix WST-1 Cell Proliferation Assay System (Takara) and expressed as an absorbance value measured using a microplate reader at 450 nm. For each measurement, wells with untreated cells and media without cells served as controls and blanks, respectively.

2.12 | Oxidized glutathione/reduced glutathione assay

To assess the oxidative stress level in tumors, we examined the GSSG/GSH ratio by using a GSSG/GSH Quantification kit (#G257; Dojindo Laboratories). Briefly, the tumor tissue (100 mg) was homogenized in lysis buffer (5% 5-sulfosalicylic acid dihydrate: #190-04572; FUJIFILM Wako Pure Chemical Corporation) and centrifuged at 8000g at 4°C for 10 min. The supernatant was collected and its absorbance value was measured using a microplate reader at 405 nm. Following the detection of GSSG, the concentration of GSH was calculated by subtracting 2×GSSG concentration from the total glutathione concentration. The GSSG/GSH ratio was determined using these parameters.

2.13 | RNA sequencing and GSEA

Total RNA extracted from BACH1-knockdown cells and their controls was converted into libraries using the SureSelect Strand-Specific RNA Library Preparation kit (Agilent). Transcriptome analysis was undertaken using the next-generation sequencer HiSeq 2500 (Illumina). The generated sequence tags were mapped onto human genomic sequences (hg38). Gene Set Enrichment Analysis (version 4.1.0) software was downloaded from the websites of the Broad Institute (<http://software.broadinstitute.org/gsea/downloads.jsp>).

2.14 | Tumor implantation

All animal experiments were carried out in strict accordance with the recommendations of the Guide for the Care and Use of Laboratory Animals of the Hiroshima University Animal Research Committee (permission no. 29-58). In a xenograft model, BACH1-overexpressed 786-O cells (786-O/exBACH1) and empty vector-transfected 786-O cells (786-O/EV) (1.0×10^4) in 100 μ l HBSS were injected subcutaneously into 8-week-old female BALB/c-nu mice (Charles River). In an allograft model, BACH1-knockout RenCa cells (RenCa/Bach1-KO) and empty vector-transfected RenCa cells (RenCa/EV) (1.0×10^5) in 50 μ l HBSS and 50 μ l Matrigel (Corning) were injected subcutaneously into 8-week-old male BALB/c mice (Charles River). The estimated tumor volumes were measured weekly for 5–6 weeks using calipers and calculated as $(w^2 \times l)/2$, where w = width and l = length. The mice were killed, the tumors were excised, and their weights were measured. Tumor cells were subjected to western blotting and GSH/GSSG assay.

2.15 | In silico analysis

Clinicopathologic data of 533 ccRCC patients in the TCGA Firehose Legacy datasets were downloaded from the cBioPortal

for Cancer Genomics (<https://www.cbioportal.org>) and used for patient characteristic analyses (age, sex, pathologic T stage, tumor grade, and stage). Upon processing mRNA expression z-scores relative to diploid samples (RNA-Seq V2 RSEM), patients were divided into BACH1 mRNA-high and -normal groups. There were no “mRNA-low” cases. Kaplan–Meier analyses of disease-free and overall survival for the two groups were carried out. By using another TCGA-based Gene Expression Profiling Interactive Analysis (GEPIA) database (gepia.cancer-pku.cn) developed by Tang et al.,²⁸ 516 ccRCC patients were divided into low and high HMOX1 expression groups using a median cut-off value. Kaplan–Meier analyses of disease-free and overall survival for the two groups were undertaken.

2.16 | Statistical analysis

Multiple group comparisons were carried out using a one-way ANOVA with Dunnett's multiple comparison test. Statistical analyses were carried out using GraphPad Prism 8 (GraphPad Software Inc.; RRID: SCR_002798). Linear regression analysis, Fisher's exact test, unpaired *t*-test, χ^2 -test, and log-rank test were used to compare the two groups. In addition, univariate and multivariate Cox regression analyses were undertaken using JMP software (SAS Institute Inc.; RRID: SCR_008567). Statistically significant differences were indicated by *p* values less than 0.05. For evaluating the false positive possibility, false discovery rate-adjusted *p* values (*q* values) were also calculated for the GSEA.

3 | RESULTS

3.1 | Expression of BACH1 in nephrectomized ccRCC patients

The expression of BACH1 in tumor specimens from nephrectomized ccRCC patients was analyzed. Immunohistochemical BACH1 staining patterns of ccRCC specimens were separable as positive or negative based on the judgments of two independent uropathologists. As shown in Figure 1A, an apparent boundary between normal and tumor tissues was recognized by the BACH1 staining. Even in the tumor samples, BACH1-positive and -negative specimens were evidently distinguishable (Figure 1B). The expression of BACH1 was mainly detected in the tumor nucleoplasm and cytoplasm. Tumor specimens positive for BACH1 were obtained from 31 (40%) of 77 patients. BACH1 expression was significantly associated with high pathologic T stage, grade, and metastatic rate in ccRCC patients (Table 1). Kaplan–Meier analysis revealed worse progression-free and cancer-specific survival rates in BACH1-positive cases compared to BACH1-negative cases ($p < 0.001$ and = 0.007, respectively) (Figure 1C). The relationship between BACH1 expression and the survival rate of patients with ccRCC was further explored by referring to a public database. High BACH1 mRNA expression in

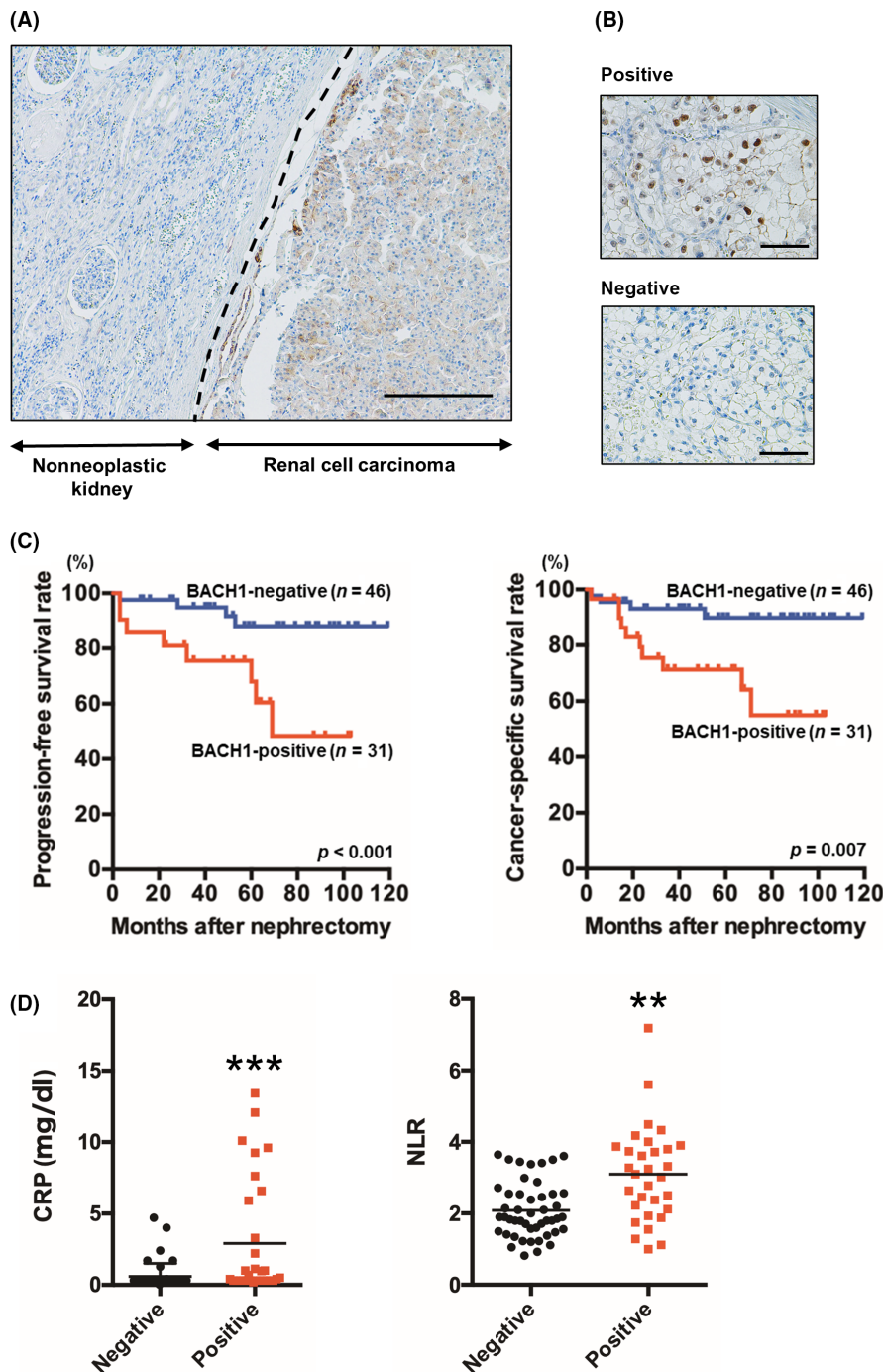


FIGURE 1 Relationship between BACH1 expression and clear cell renal cell carcinoma (ccRCC) progression. (A) Immunohistochemical BACH1 staining of nonneoplastic kidney and ccRCC. The results shown are representative of 77 independent specimens. Original magnification, $\times 100$. Scale bar, 200 μm . Broken line indicates the boundary between nonneoplastic and cancerous tissue. (B) Immunohistochemical staining of BACH1-positive and -negative tumors. The results shown are representative of 31 BACH1-positive and 46 BACH1-negative specimens. Original magnification, $\times 400$. Scale bar, 50 μm . (C) Kaplan-Meier plots of progression-free (left) and cancer-specific (right) survival rates for BACH1-positive and -negative nephrectomized ccRCC patients. p values calculated by a log-rank test are also indicated. (D) Serum C-reactive protein (CRP) and neutrophil-to-lymphocyte ratio (NLR) levels in BACH1-positive ($n = 31$) and -negative ccRCC ($n = 46$) patients. $*p < 0.05$ and $**p < 0.001$ by unpaired t -test, compared with BACH1-negative patients.

ccRCC patients was significantly associated with high pathologic T and disease stages (Table S2). Furthermore, disease-free and overall survival rates were significantly worse in BACH1 mRNA-high cases than in BACH1 mRNA-normal cases ($p = 0.013$ and 0.002 , respectively; Figure S1). These results suggest that BACH1 expression is associated with poor prognosis in patients with ccRCC.

Next, we evaluated the association between BACH1 expression and serum inflammatory marker levels. Serum levels of CRP and the NLR were significantly higher in BACH1-positive cases than in BACH1-negative cases (Figure 1D), suggesting a relationship between BACH1 expression and inflammatory responses.

3.2 | BACH1 promotes cell invasion and migration, but not proliferation, in vitro

To determine the functional significance of BACH1 in RCC, we investigated the contribution of BACH1 to cell invasion, migration, and proliferation by knocking down and overexpressing BACH1 in 786-O, Caki-1, and ACHN cells, well-known RCC cell lines.²⁹ Successful knockdown (Figure 2A) and overexpression (Figure 2B) of BACH1 were confirmed at the mRNA (Figure 2A,B, upper panels) and protein (Figure 2A,B, lower panels) levels by qRT-PCR and western blotting, respectively. BACH1-knockdown

TABLE 1 Comparison of clinical characteristics between BACH1-positive and -negative nephrectomized clear cell renal cell carcinoma patients

	Case (% of total)		p value
	BACH1-positive (n = 31)	BACH1-negative (n = 46)	
Age, years			
≤70	22 (71.0)	29 (63.0)	0.47
>70	9 (29.0)	17 (37.0)	
Gender			
Male	24 (77.4)	34 (73.9)	0.72
Female	7 (22.6)	12 (26.1)	
Pathologic T stage			
<pT3	18 (58.1)	40 (87.0)	<0.01
≥pT3	13 (41.9)	6 (13.0)	
Tumor grade			
G1/2	16 (51.6)	36 (78.3)	0.01
G3	15 (48.4)	10 (21.7)	
Lymph node status			
N0	26 (83.9)	43 (93.5)	0.18
N1	5 (16.1)	3 (6.5)	
Metastasis status			
M0	19 (61.3)	43 (93.5)	<0.01
M1	12 (38.7)	3 (6.5)	

and -overexpressed cells displayed significantly decreased and increased invasive activity, respectively, compared to their controls (Figure 2C,D). In addition, the migration activity of 786-O, Caki-1, and ACHN cells was downregulated and upregulated by knockdown and overexpression of BACH1, respectively (Figure 2E,F). However, the proliferation of these cells was not affected by knockdown or overexpression of BACH1 (Figure S2), suggesting that BACH1 promotes RCC cell invasion and migration without affecting proliferative activity in vitro.

To investigate the role of BACH1 in the expression of OSR-related proteins, western blotting for p21, p53, and RB was carried out onto BACH1-overexpressed 786-O and Caki-1 cells. The expression of p53 and RB was not affected but that of p21 was slightly downregulated by BACH1 overexpression (Figure S3).

3.3 | RNA sequencing analysis for BACH1-knockdown cells

We undertook RNA sequencing analysis of BACH1-knockdown 786-O cells. Upon processing the resulting data with GSEA, a series of hallmark gene sets were extracted (Figure 3A). Among several notable pathways extracted, inflammatory response, EMT, mTORC1 signaling, and angiogenesis pathways, as well as 13 other pathways, were significantly associated with the expression of BACH1 (Figure 3B–E).

3.4 | BACH1 regulates HO-1 in RCC

BACH1 binds to the antioxidant response element of the *HMOX1* promoter and consequently inhibits its gene transcription under homeostatic conditions.³⁰ To explore the possibility that BACH1 is related to the poor prognosis of RCC through the suppression of HO-1, we analyzed HO-1 expression in BACH1-knockdown and BACH1-overexpressed 786-O, Caki-1, and ACHN cells. The expression of HO-1 was increased and decreased in BACH1-knockdown (Figure 4A) and BACH1-overexpressed cells (Figure 4B), respectively, at mRNA (Figure 4A,B, upper panels) and protein (Figure 4A,B, lower panels) levels. These findings suggested that BACH1 negatively regulates HO-1 expression in RCC cells.

Next, we analyzed the expression of HO-1 in tumor specimens from nephrectomized ccRCC patients. Immunohistochemical staining showed that HO-1 was mainly detected in the cytoplasm and cell membranes of ccRCC tissues at different levels. Upon grading the HO-1 staining levels as very weak, weak, moderate, and strong, we divided cases with very weak and weak grades into the HO-1-low group and those with moderate and strong grades in the HO-1-high group (Figure 4C). Of the 77 examined cases, 23% were categorized into the HO-1-high group. The expression of HO-1 was negatively associated with a high pathologic T stage (Table 2). In addition, the progression-free survival rate tended to be poor in the HO-1-low group (Figure 4D), although there was no difference in the cancer-specific survival rate between the two groups (Figure 4E). The relationship between *HMOX1* expression and the survival rate of patients with ccRCC was further explored by referring to a public database. Results from the database showed that disease-free and overall survival rates were significantly worse in *HMOX1* mRNA-low cases than in mRNA-high cases ($p = 0.001$ and <0.001 , respectively; Figure S4).

The immunohistochemical staining of HO-1 tended to be weaker and stronger in BACH1-positive and -negative tumors, respectively (Figure 4F). The staining intensity grading data further indicated a negative correlation between BACH1 and HO-1 expression ($p = 0.029$; Table 3). In contrast to BACH1, HO-1 expression was observed in tumor-adjacent normal tissues to some degree, even though the spontaneous HO-1 expression did not show a significant correlation with tumor BACH1 expression (Table S3). These findings suggest that BACH1-mediated poor prognosis in ccRCC patients is related, at least in part, to the downregulation of HO-1.

3.5 | BACH1 regulates tumor progression in vivo

To examine the role of BACH1 in tumor progression in vivo, a xenograft model was generated by subcutaneous implantation of 786-O/EV and 786-O/exBACH1 cells into BALB/c-nu mice. The estimated volumes of 786-O/exBACH1 tumors were significantly larger than those of 786-O/EV tumors at 14, 21, 28, and 42 days after transplantation (Figure 5A). At the end-point, 786-O/exBACH1 tumors were mostly larger and significantly heavier than 786-O/EV tumors (Figure 5B).

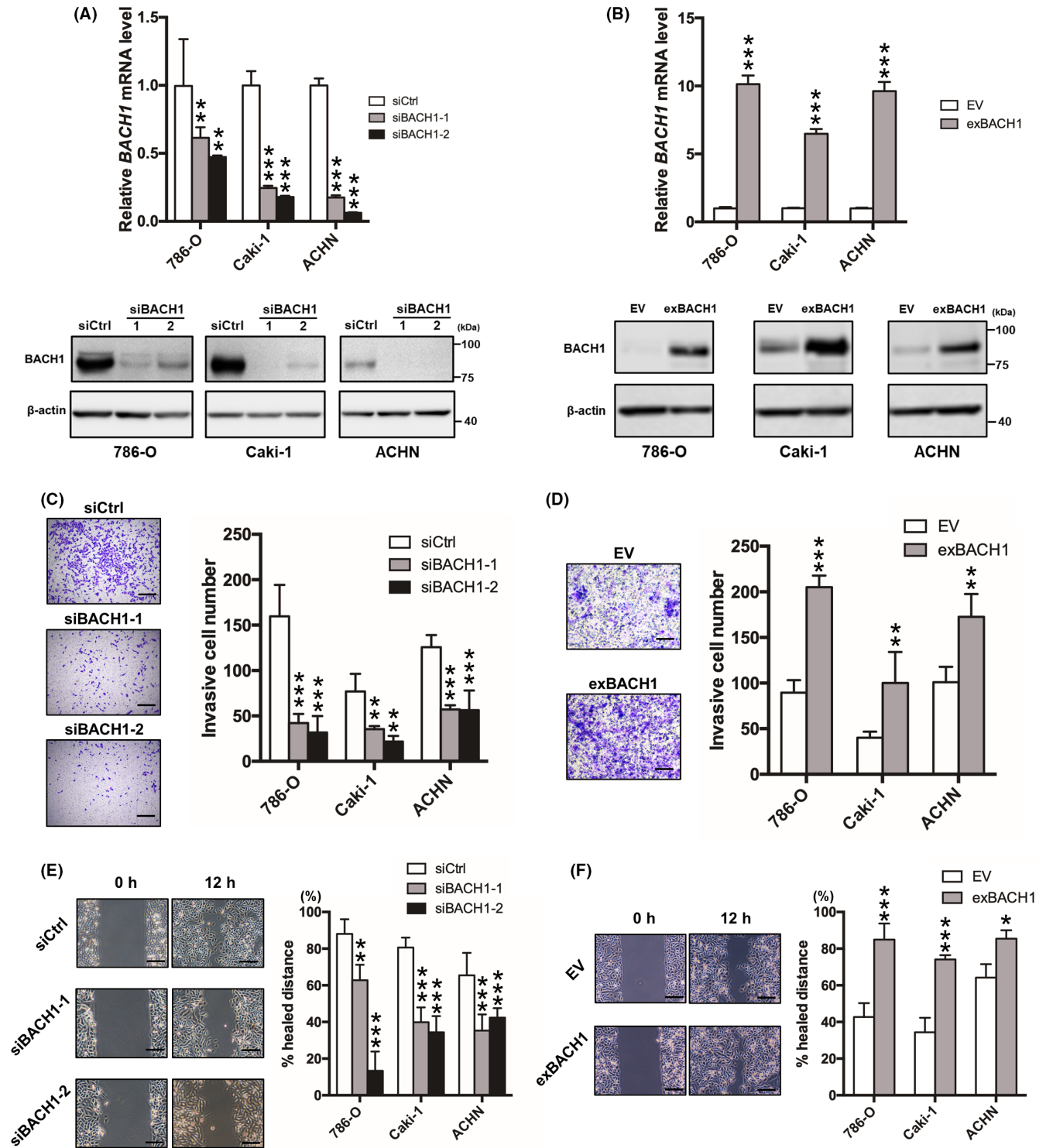
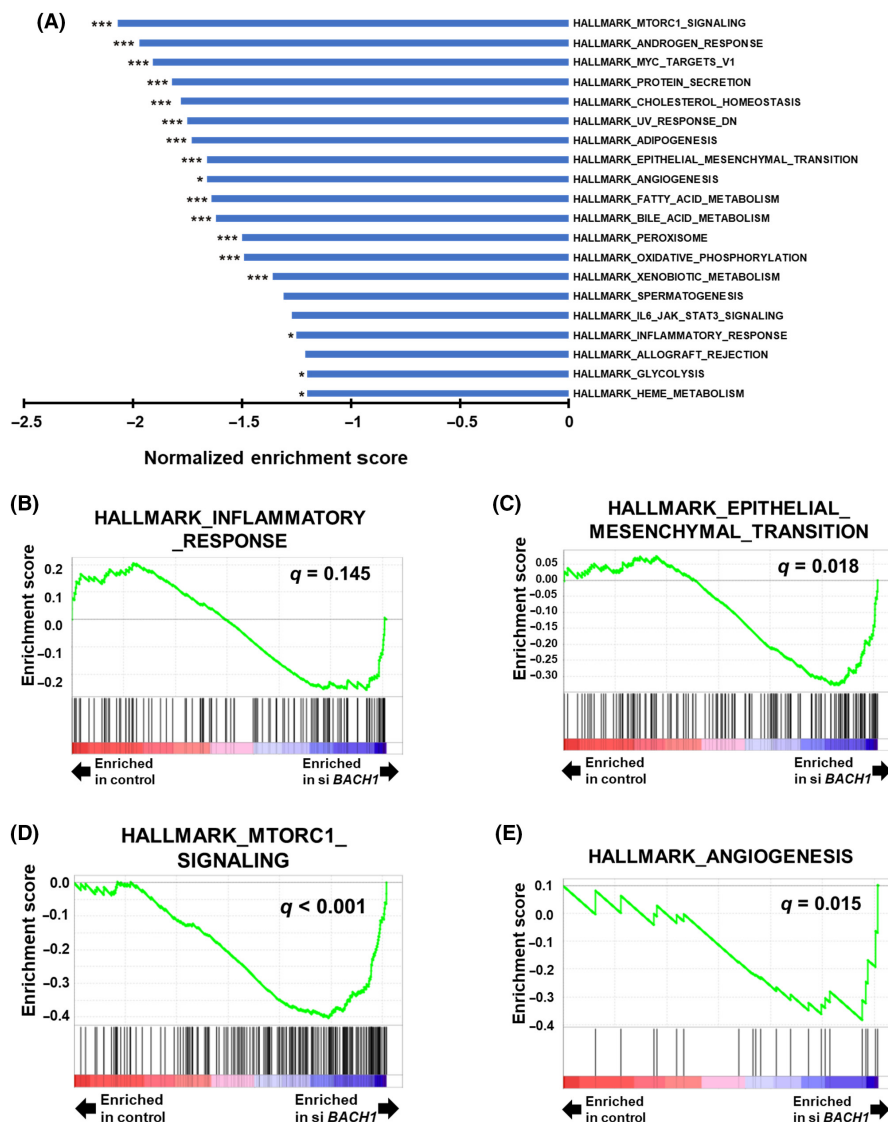


FIGURE 2 Role of BACH1 in renal cell carcinoma cell invasion and migration in vitro. (A) BACH1-knockdown (siBACH1-1 and siBACH1-2) and (B) -overexpressed (exBACH1) 786-O, Caki-1, and ACHN cells were subjected to determine mRNA (upper panels) and protein (lower panels) levels of BACH1 by quantitative RT-PCR and western blot analysis, respectively. Results are expressed as mean \pm SEM (upper panels) or representative of three experiments. $**p < 0.01$ and $***p < 0.001$ by one-way ANOVA combined with Dunnett's multiple comparisons test, compared with control siRNA-introduced control (siCtrl) or empty vector-introduced control (EV). (C) BACH1-knockdown and (D) BACH1-overexpressed cell lines were subjected to Transwell invasion assay with corresponding control cells (siCtrl or EV) ($n = 4$). $**p < 0.01$ and $***p < 0.001$ by one-way ANOVA combined with Dunnett's multiple comparisons test, compared with siCtrl or EV. Representative Diff-Quick-stained Transwell membranes using 786-O cells are shown in left panels. Scale bar, 50 μ m. (E) BACH1-knockdown and (F) BACH1-overexpressed cell lines were subjected to wound healing assay with corresponding control cells (siCtrl or EV) ($n = 3$). $*p < 0.05$, $**p < 0.01$, and $***p < 0.001$ by one-way ANOVA combined with Dunnett's multiple comparisons test, compared with siCtrl or EV. Representative images of migrated cells using 786-O cells are shown in left panels. Scale bar, 50 μ m.

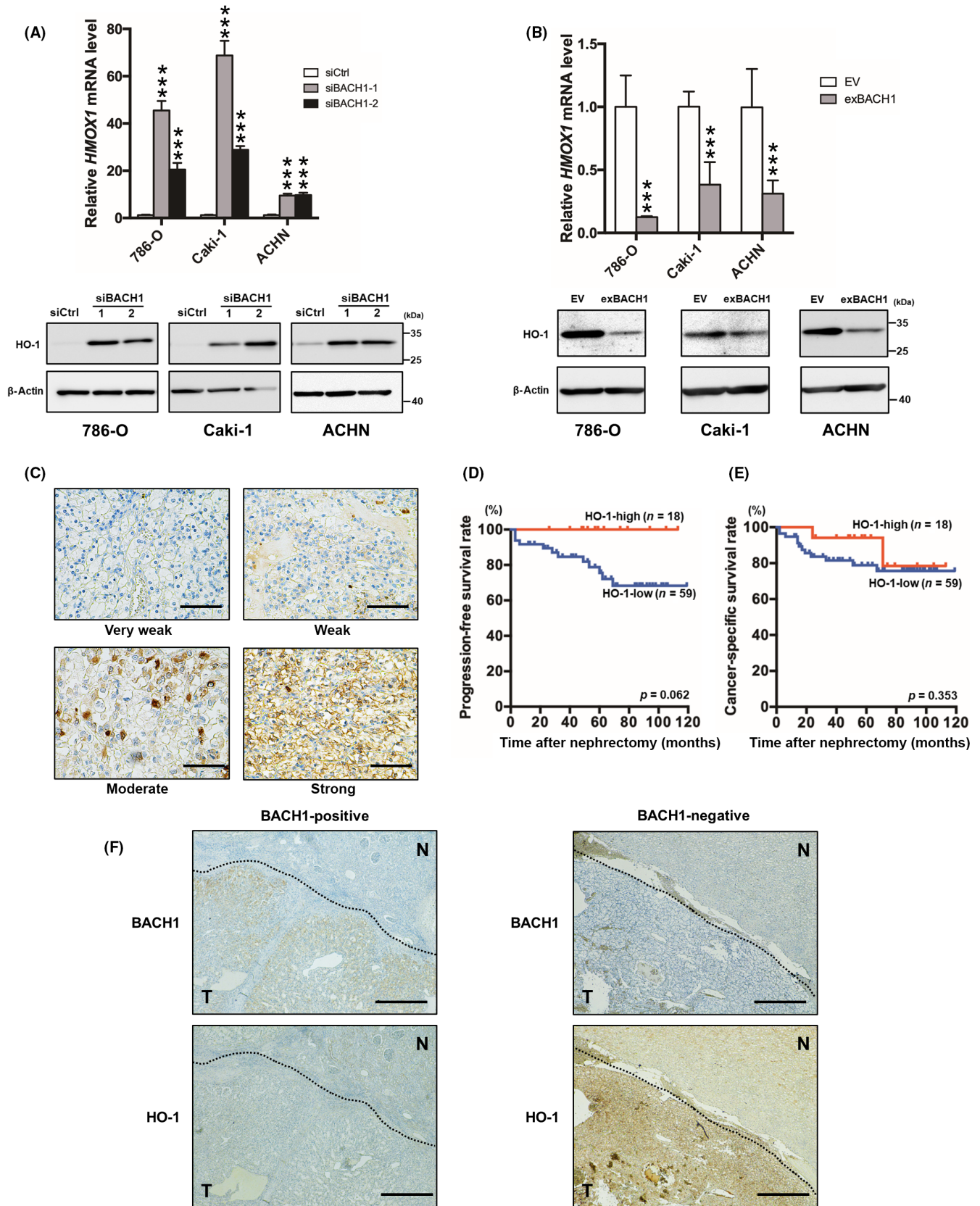
FIGURE 3 Gene Set Enrichment Analysis (GSEA) of BACH1-knockdown renal cell carcinoma cells. (A) Normalized enrichment scores of the top 20 downregulated pathways of hallmark gene sets enriched in BACH1-knockdown 786-O cells. * $p < 0.05$ and *** $p < 0.001$, compared with control siRNA-introduced control. (B) Enrichment pattern of hallmark inflammatory response-related, (C) epithelial-mesenchymal transition-related, (D) mTORC1 signaling-related, and (E) angiogenesis-related gene sets determined by GSEA comparing BACH1-knockdown (siBACH1) and control cells. q values are also indicated.



We further generated an allograft model by subcutaneous implantation of RenCa/EV and RenCa/Bach1-KO cells into BALB/c mice after confirming the knockout of Bach1 (Figure S5). Consistent with the results of BACH1 overexpression in a xenograft model, the estimated volumes of RenCa/Bach1-KO tumors were significantly smaller than those of RenCa/EV tumors at 21, 28, and 35 days after transplantation (Figure 5C). At the end-point, RenCa/Bach1-KO tumors were mostly smaller and significantly lighter than RenCa/EV tumors (Figure 5D).

Epithelial-mesenchymal transition is characterized by downregulation of the epithelial cell marker E-cadherin, followed by upregulation of mesenchymal cell markers, including N-cadherin and vimentin.³¹ Consistent with the involvement of BACH1 in the EMT-related pathway (Figure 3C), reduced expression of E-cadherin and increased expression of N-cadherin and vimentin were detected in 786-O/exBACH1 tumors following the augmentation of BACH1 expression (Figure 5E). In contrast to the in vivo results, an almost

FIGURE 4 Relationship between BACH1 and heme oxygenase-1 (HO-1) expression. (A) BACH1-knockdown (siBACH1-1 and siBACH1-2) and (B) -overexpressed (exBACH1) 786-O, Caki-1, and ACHN cells were subjected to determine *HMOX1* mRNA (upper panels) and HO-1 protein (lower panels) levels by quantitative RT-PCR and western blot analysis, respectively. Results are expressed as mean \pm SEM (upper panels) or representative of three experiments. *** $p < 0.001$, compared with control siRNA-introduced control (siCtrl) or empty vector-introduced control (EV) by one-way ANOVA combined with Dunnett's multiple comparisons test. (C) Immunohistochemical HO-1 staining of clear cell renal cell carcinoma (ccRCC) specimens categorized into four grades; very weak, weak, moderate, and strong. The results shown are representative of 77 independent specimens. Original magnification, $\times 400$. Scale bar, 50 μ m. (D) Kaplan-Meier plots of progression-free and (E) cancer-specific survival rates for HO-1-high and -low nephrectomized ccRCC patients. p values calculated by a log-rank test are also indicated. (F) Immunohistochemical BACH1 (upper panels) and HO-1 (lower panels) staining of BACH1-positive (left panels) and -negative (right panels) ccRCC specimens in the continuous sections. Results shown are representative of 30 BACH1-positive and 47 BACH1-negative specimens. N, normal area; T, tumor area. Original magnification, $\times 100$. Scale bar, 200 μ m.



undetectable basal expression of E-cadherin protein (data not shown) and the ineffectiveness of BACH1 overexpression on the weak mRNA expression of *CDH1*, an E-cadherin coding gene, was

observed in 786-O cells in vitro (Figure S6). To prove the association between BACH1 and OSRs in the developed tumor, we assessed the ratio of oxidized and reduced glutathione levels. The GSSG/GSH

ratio was significantly downregulated in RenCa/Bach1-KO tumors (Figure 5F). These findings suggest that BACH1 contributes to RCC progression *in vivo*, in relation to OSRs with the activation of EMT-related pathways.

4 | DISCUSSION

Various biological processes related to OSRs have been strongly implicated in the development and prognosis of several types of cancer. However, the critical contribution of OSRs to RCC has not yet been thoroughly investigated. This study revealed the close interaction of BACH1, a representative OSR-related transcription factor, with the prognosis of nephrectomized ccRCC patients. The expression of

BACH1 in ccRCC tissues was correlated with poor prognosis and serum inflammatory markers such as CRP and NLR, providing a reasonable explanation for previous studies describing the potential of these markers for predicting the prognosis of RCC patients.³²⁻³⁴ The significant participation of BACH1 in OSR-related GSSG/GSH ratio upregulation was demonstrated in the allograft model. As observed in other solid types of cancer^{35,36} BACH1 significantly contributes to the increased invasion and migration ability of RCC cell lines without affecting their proliferation *in vitro*. In addition, BACH1 plays a role in tumor progression in relation to enhanced EMT-related responses *in vivo*.

The relationship between the expression of BACH1 and worse prognosis in solid cancers has been reported in pancreatic, esophageal, lung, and ovarian cancers.³⁵⁻³⁹ Consistently, we showed the potential usefulness of BACH1 expression in predicting the prognosis of patients with ccRCC with its corresponding cellular mechanisms. Furthermore, we elucidated the involvement of BACH1-mediated HO-1 downregulation in the worse survival trend of patients with ccRCC. Heme oxygenase-1 has been identified in several types of cancer; however, the role of HO-1 in tumor progression is currently being debated.^{23,40-42} Even in ccRCC cases, Deng et al.⁴² reported worse prognosis in patients with high HO-1 expression. Although the differences in the background of patients included and experimental conditions need to be considered, our present findings suggest that HO-1 contributes negatively to tumor progression both in our own patient samples and public databases. The antioxidant activity of HO-1 is related to its cytoprotective effect through the clearance of intracellular toxic heme.⁴³ However, this process also positively modulates the tumor microenvironment, partly by facilitating angiogenesis and metastasis.^{44,45} Pharmacological inhibition of HO-1 has been proposed to enhance antitumor immune responses.⁴⁰ Although further studies are needed to elucidate this discrepancy, loss of antioxidant activity rather than tumor microenvironment progression or immune response suppression could be essential, at least for the poor prognosis of HO-1-low ccRCC patients.

Consistent with the results of the serum marker analysis for ccRCC patients and GSEA for BACH1-knockdown cells, indicating the association between BACH1 and inflammation, the invasion and migration of RCC cell lines were regulated by BACH1. These *in vitro* findings were supported by *in vivo* xenograft experiments showing downregulation of E-cadherin in BACH1-overexpressed tumors. Thus, the loss of E-cadherin-mediated cell adhesion likely contributes to the

TABLE 2 Comparison of clinical characteristics between HO-1-high and -low nephrectomized clear cell renal cell carcinoma patients

	Case (% of total)		p value
	HO-1-high (n = 18)	HO-1-low (n = 59)	
Age, years			
≤70	9 (50.0)	42 (71.2)	0.10
>70	9 (50.0)	17 (28.8)	
Gender			
Male	13 (72.2)	45 (76.3)	0.73
Female	5 (27.8)	14 (23.7)	
Pathologic T stage			
<pT3	17 (94.4)	41 (69.5)	0.02
≥pT3	1 (5.6)	18 (30.5)	
Tumor grade			
G1/2	15 (83.3)	37 (62.7)	0.08
G3	3 (16.7)	22 (37.3)	
Lymph node status			
N0	16 (88.9)	53 (89.8)	0.91
N1	2 (11.1)	6 (10.2)	
Metastasis status			
M0	16 (88.9)	43 (78.0)	0.28
M1	2 (11.1)	13 (22.0)	

TABLE 3 Relationship between BACH1 and heme oxygenase-1 (HO-1) expression in nephrectomized clear cell renal cell carcinoma patients

HO-1 (tumor tissue)	Percentage		p value
	BACH1-positive	BACH1-negative	
Very weak	63.3	51.1	0.029
Weak	23.3	19.1	
Moderate	10.0	19.1	
Strong	3.4	10.7	

Note: Based on immunohistochemical staining of tumor specimens, patients were categorized into positive and negative for BACH1 and very weak, weak, moderate, and strong for HO-1. Results are expressed as the percentage of BACH1-positive (n = 30) and -negative (n = 47) patients. The p value was calculated using the χ^2 -test.

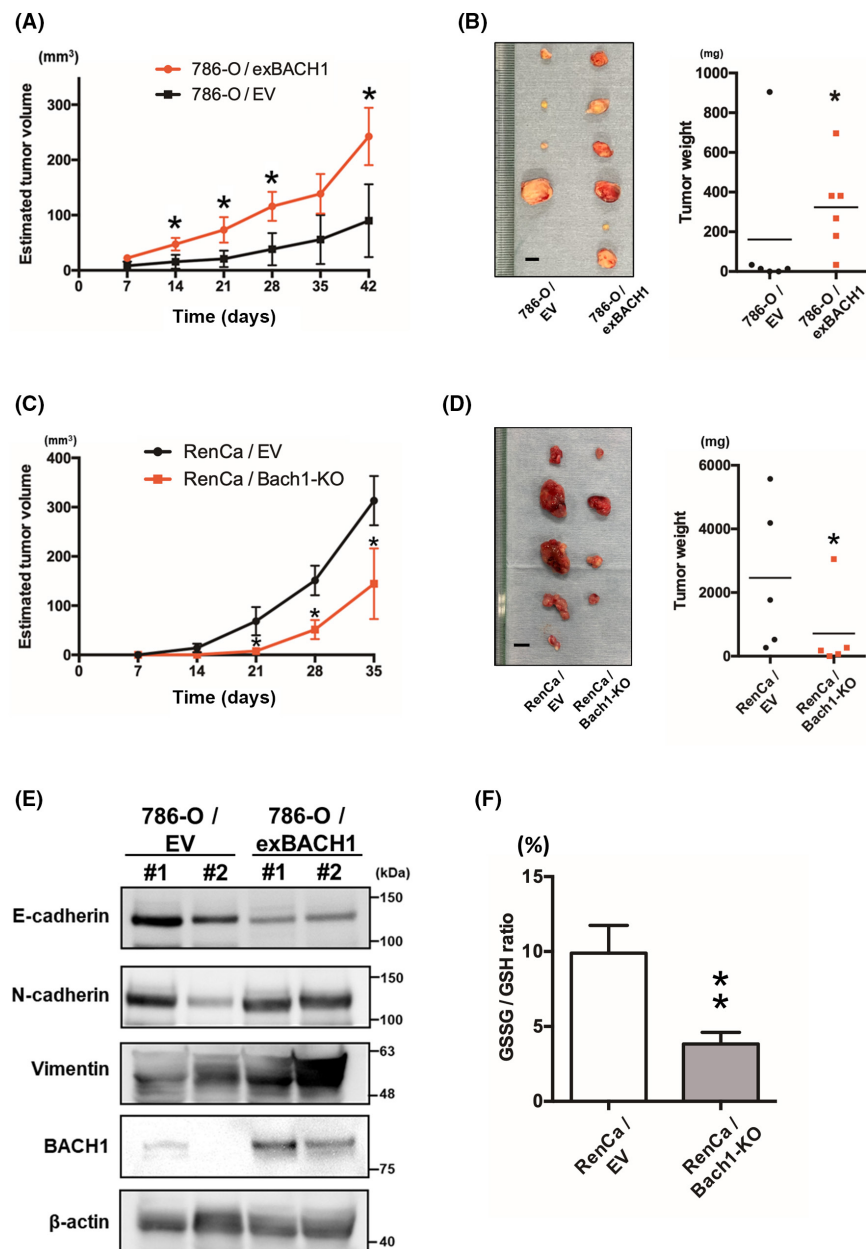


FIGURE 5 Role of BACH1 in tumor progression in vivo. (A) Estimated tumor volume of empty vector-introduced (786-O/EV) and BACH1-overexpressed (786-O/exBACH1) 786-O cell-transplanted mice ($n = 6$). Results are expressed as the mean \pm SEM. * $p < 0.05$ by unpaired t-test, compared with 786-O/EV. (B) Photographic data (left panel) and weight (right panel) of excised 786-O/EV and 786-O/exBACH1 tumors at the end-point ($n = 6$). Scale bar, 5 mm (left panel). * $p < 0.05$ by unpaired t-test, compared with EV. (C) Estimated tumor volume of empty vector-introduced (RenCa/EV) and Bach1-knockout (RenCa/Bach1-KO) RenCa cell-transplanted mice ($n = 5$). Results are expressed as mean \pm SEM. * $p < 0.05$ by unpaired t-test, compared with RenCa/EV. (D) Photographic data (left panel) and weight (right panel) of excised RenCa/EV and RenCa/Bach1-KO tumors at the end-point ($n = 5$). Scale bar, 5 mm (left panel). * $p < 0.05$ by unpaired t-test, compared with RenCa/EV. (E) Top two tumor samples in (B) left panel were subjected to western blot analysis for E-cadherin, N-cadherin, vimentin, BACH1, and β -actin. (F) Comparison of the oxidized glutathione/reduced glutathione (GSSG/GSH) ratio of RenCa/EV and RenCa/Bach1-KO tumors. ** $p < 0.01$ by unpaired t-test, compared with RenCa/EV.

initiation of RCC cell invasion.^{46,47} Furthermore, through the downregulation and upregulation of FOXA1 and Snail family transcriptional repressor 2, respectively, BACH1 has been reported to suppress the expression of *CDH1*.^{18,35,48} The direct interaction of FOXA1 with the *CDH1* promoter was reported, although that of BACH1 has not been determined. Further studies are required to confirm the corresponding mechanisms involved in RCC cells and patients.

In contrast to its crucial participation in invasion and migration, the proliferation of RCC cells was not affected by BACH1 in vitro. This is partly contradictory to and partly consistent with the study by Sato et al.,³⁵ indicating the functional role of BACH1 in proliferation-related gene expression, regardless of its dispensable role in the proliferation of pancreatic ductal adenocarcinoma cells. This study reported the lack of enrichment of proliferation-related pathways in BACH1-knockdown 786-O cells, suggesting the differential contribution of BACH1 among cell and cancer types.

In particular, with the apparent contradiction to the in vitro results, the tumor growth of RCC cells in vivo was upregulated and downregulated by overexpression and knockout of BACH1, respectively. In contrast to the partial downregulation of OSR-related pathways, such as p21 expression, by BACH1 overexpression in vitro, decreased GSSG/GSH ratio was observed in Bach1 KO tumors in vivo. As BACH1 forms a complex with p53 and resultingly inhibits a part of its function,⁴⁹ BACH1 could play a competitive role in p53-mediated p21 expression. These in vitro and in vivo experiments were essentially different under the cell-surrounding conditions. In fact, the expression of the *CDH1* gene products was very low in 786-O cells and not affected by BACH1 overexpression in vitro. Therefore, BACH1-overexpressed cells displayed enhanced proliferative potential, probably through interactions with their surrounding microenvironments. Angiogenesis is one of the most important OSR-related physiological processes induced in tumor-surrounding

microenvironments. This process does not occur in cancer cells alone; for example, in vitro culture conditions, although it is essential for the growth of most types of solid tumors and, consequently, is often a rate-limiting step of cancer proliferation in vivo.¹¹ Consistent with our present findings revealing BACH1 involvement in the angiogenesis pathway, the enhancement of angiogenesis by BACH1 through upregulation of VEGF was previously reported in esophageal, ovarian, and colorectal cancers.^{36,50,51} Several TKIs for the tyrosine kinases that are involved in the downstream pathways of VEGF receptors have been used for advanced RCC treatment. Furthermore, a relationship between BACH1 and CD31 expression, another angiogenesis-related cell adhesion molecule, has been reported.³⁶ Together, it was suggested that BACH1 participates in tumor progression at the invasion, migration, and proliferation processes in vivo mainly through its functional role in cancer cells and their surrounding microenvironment.

Remarkably, BACH1 was associated with the mTOR signaling pathway, which is also related to OSRs⁵² and a target of conventional RCC therapeutic agents, mTOR inhibitors. Although the detailed causal relationship should be further explored, the expression level of BACH1 could correlate with the therapeutic responses of patients with RCC to mTOR inhibitors and TKIs.

In summary, BACH1 expression is associated with poor prognosis in nephrectomized ccRCC patients. In addition to the involvement of HO-1 suppression, the contribution of inflammation-, EMT-, and angiogenesis-related upregulation of cellular invasion, migration, and proliferation to BACH1-mediated tumor progression was suggested. BACH1 could be a biomarker for predicting the effectiveness of mTOR inhibitors and TKIs in patients with ccRCC.

AUTHOR CONTRIBUTIONS

Conception and design: K. Takemoto, K. Kobatake. Development of methodology: K. Takemoto, K. Kobatake, K. Miura. Acquisition of data (provided animals, acquired and managed patients, provided facilities, etc.): K. Takemoto, K. Kobatake, K. Miura, T. Fukushima, T. Babasaki, S. Miyamoto, Y. Sekino, H. Kitano, K. Goto, K. Ikeda, K. Hieda, T. Hayashi. Analysis and interpretation of data (e.g., statistical analysis, biostatistics, computational analysis): K. Takemoto, K. Kobatake, K. Miura, Y. Sekino, K. Goto, K. Ikeda. Writing, review, and/or revision of the manuscript: K. Takemoto, K. Kobatake, K. Miura, Y. Sekino, K. Goto, K. Ikeda, N. Hinata, O. Kaminuma. Administrative, technical, or material support (i.e., reporting or organizing data, constructing databases): K. Takemoto, K. Kobatake, K. Miura, T. Babasaki, Y. Sekino, K. Goto, K. Ikeda. Study supervision: K. Kobatake, N. Hinata, O. Kaminuma.

ACKNOWLEDGMENTS

This work was in part supported by JSPS KAKENHI (grant number 21K09426) and funded by a Joint Research Grant from the Research Center for Radiation Disaster Medical Science to K.K. We thank Norimasa Yamasaki, Sawako Ogata, and Kohei Kawai for assistance with experiments and animal care. We also would like to thank Editage for English language editing.

DISCLOSURE

The authors have no conflict of interest.

ETHICS STATEMENT

Approval of the research protocol by an institutional review board: All experimental procedures were performed according to the ethical standards of the Declaration of Helsinki and were approved by the Ethics Committee of Hiroshima University Hospital (approval no. E-588-2).

Animal studies: All animal experiments were carried out in strict accordance with the recommendations of the Guide for the Care and Use of Laboratory Animals of the Hiroshima University Animal Research Committee (permission no. 29-58).

ORCID

Kenshiro Takemoto  <https://orcid.org/0000-0002-9077-4733>

Kohei Kobatake  <https://orcid.org/0000-0003-2098-3916>

Nobuyuki Hinata  <https://orcid.org/0000-0001-7014-6812>

REFERENCES

- Sung H, Ferlay J, Siegel RL, et al. Global Cancer Statistics 2020: GLOBOCAN estimates of incidence and mortality worldwide for 36 cancers in 185 countries. *CA Cancer J Clin.* 2021;71:209-249.
- Lalani A-KA, McGregor BA, Albiges L, et al. Systemic treatment of metastatic clear cell renal cell carcinoma in 2018: current paradigms, use of immunotherapy, and future directions. *Eur Urol.* 2019;75:100-110.
- Choueiri TK, Motzer RJ. Systemic therapy for metastatic renal-cell carcinoma. *N Engl J Med.* 2017;376:354-366.
- Chow W-H, Dong LM, Devesa SS. Epidemiology and risk factors for kidney cancer. *Nat Rev Urol.* 2010;7:245-257.
- Capitanio U, Bensalah K, Bex A, et al. Epidemiology of renal cell carcinoma. *Eur Urol.* 2019;75:74-84.
- Benichou J, Chow WH, McLaughlin JK, Mandel JS, Fraumeni JF. Population attributable risk of renal cell cancer in Minnesota. *Am J Epidemiol.* 1998;148:424-430.
- Hsieh JJ, Purdue MP, Signoretti S, et al. Renal cell carcinoma. *Nat Rev Dis Primers.* 2017;3:17009.
- Dey S, Hamilton Z, Noyes SL, et al. Chronic kidney disease is more common in locally advanced renal cell carcinoma. *Urology.* 2017;105:101-107.
- Eltzschig HK, Carmeliet P. Hypoxia and inflammation. *N Engl J Med.* 2011;364:656-665.
- Coussens LM, Werb Z. Inflammation and cancer. *Nature.* 2002;420:860-867.
- Hanahan D, Weinberg RA. Hallmarks of cancer: the next generation. *Cell.* 2011;144:646-674.
- Prasad S, Gupta SC, Tyagi AK. Reactive oxygen species (ROS) and cancer: role of antioxidative nutraceuticals. *Cancer Lett.* 2017;387:95-105.
- Diakos CI, Charles KA, McMillan DC, Clarke SJ. Cancer-related inflammation and treatment effectiveness. *Lancet Oncol.* 2014;15:e493-e503.
- Hayes JD, Dinkova-Kostova AT, Tew KD. Oxidative stress in cancer. *Cancer Cell.* 2020;38:167-197.
- Li G, Ding K, Qiao Y, et al. Flavonoids regulate inflammation and oxidative stress in cancer. *Molecules.* 2020;25:5628.
- Chikara S, Nagaprashantha LD, Singhal J, Horne D, Awasthi S, Singhal SS. Oxidative stress and dietary phytochemicals: role in cancer chemoprevention and treatment. *Cancer Lett.* 2018;413:122-134.

17. Chang Y, An H, Xu L, et al. Systemic inflammation score predicts postoperative prognosis of patients with clear-cell renal cell carcinoma. *Br J Cancer*. 2015;113:626-633.
18. Igarashi K, Nishizawa H, Saiki Y, Matsumoto M. The transcription factor BACH1 at the crossroads of cancer biology: from epithelial-mesenchymal transition to ferroptosis. *J Biol Chem*. 2021;297:101032.
19. Oyake TIK, Motohashi H, Hayashi N, et al. Bach proteins belong to a novel family of BTB-basic leucine zipper transcription factors that interact with MafK and regulate transcription through the NF-E2 site. *Mol Cell Biol*. 1996;16:6083-6095.
20. Zhang X, Guo J, Wei X, et al. Bach1: function, regulation, and involvement in disease. *Oxid Med Cell Longev*. 2018;2018:1-8.
21. Wiel C, Le Gal K, Ibrahim MX, et al. BACH1 stabilization by antioxidants stimulates lung cancer metastasis. *Cell*. 2019;178:330-345.e322.
22. Igarashi K, Kurosaki T, Roychoudhuri R. BACH transcription factors in innate and adaptive immunity. *Nat Rev Immunol*. 2017;17:437-450.
23. Chiang S-K, Chen S-E, Chang L-C. The role of HO-1 and its crosstalk with oxidative stress in cancer cell survival. *Cell*. 2021;10:2401.
24. Moch H, Cubilla AL, Humphrey PA, Reuter VE, Ulbright TM. The 2016 WHO classification of tumours of the urinary system and male genital organs—part a: renal, penile, and testicular tumours. *Eur Urol*. 2016;70:93-105.
25. Edge SB, Compton CC. The American Joint Committee on Cancer: the 7th Edition of the AJCC cancer staging manual and the future of TNM. *Ann Surg Oncol*. 2010;17:1471-1474.
26. Tetsutaro Hayashi AM, Ohara S, Mita K, et al. Immunohistochemical analysis of Reg IV in urogenital organs: frequent expression of Reg IV in prostate cancer and potential utility as serum tumor marker. *Oncol Rep*. 2009;21(1):95-100.
27. Sekino Y, Han X, Babasaki T, et al. TUBB3 is associated with high-grade histology, poor prognosis, p53 expression, and cancer stem cell markers in clear cell renal cell carcinoma. *Oncology*. 2020;98:689-698.
28. Tang Z, Li C, Kang B, Gao G, Li C, Zhang Z. GEPIA: a web server for cancer and normal gene expression profiling and interactive analyses. *Nucleic Acids Res*. 2017;45:W98-W102.
29. Brodaczevska KK, Szczylik C, Fiedorowicz M, Porta C, Czarnecka AM. Choosing the right cell line for renal cell cancer research. *Mol Cancer*. 2016;15:83.
30. Campbell NK, Fitzgerald HK, Dunne A. Regulation of inflammation by the antioxidant haem oxygenase 1. *Nat Rev Immunol*. 2021;21:411-425.
31. Dongre A, Weinberg RA. New insights into the mechanisms of epithelial-mesenchymal transition and implications for cancer. *Nat Rev Mol Cell Biol*. 2019;20:69-84.
32. Pichler M, Hutterer GC, Stoeckigt C, et al. Validation of the pre-treatment neutrophil-lymphocyte ratio as a prognostic factor in a large European cohort of renal cell carcinoma patients. *Br J Cancer*. 2013;108:901-907.
33. Chen X, Meng F, Jiang R. Neutrophil-to-lymphocyte ratio as a prognostic biomarker for patients with metastatic renal cell carcinoma treated with immune checkpoint inhibitors: a systematic review and meta-analysis. *Front Oncol*. 2021;11:746976.
34. Steffens S, Köhler A, Rudolph R, et al. Validation of CRP as prognostic marker for renal cell carcinoma in a large series of patients. *BMC Cancer*. 2012;12:399.
35. Sato M, Matsumoto M, Saiki Y, et al. BACH1 promotes pancreatic cancer metastasis by repressing epithelial genes and enhancing epithelial-mesenchymal transition. *Cancer Res*. 2020;80:1279-1292.
36. Zhao Y, Gao J, Xie X, et al. BACH1 promotes the progression of esophageal squamous cell carcinoma by inducing the epithelial-mesenchymal transition and angiogenesis. *Cancer Med*. 2021;10:3413-3426.
37. Lignitto L, Leboeuf SE, Homer H, et al. Nrf2 activation promotes lung cancer metastasis by inhibiting the degradation of Bach1. *Cell*. 2019;178:316-329.e318.
38. Han W, Zhang Y, Niu C, et al. BTB and CNC homology 1 (Bach1) promotes human ovarian cancer cell metastasis by HMGA2-mediated epithelial-mesenchymal transition. *Cancer Lett*. 2019;445:45-56.
39. Jiang P, Li F, Liu Z, Hao S, Gao J, Li S. BTB and CNC homology 1 (Bach1) induces lung cancer stem cell phenotypes by stimulating CD44 expression. *Respir Res*. 2021;22:320.
40. Luu Hoang KN, Anstee JE, Arnold JN. The diverse roles of heme oxygenase-1 in tumor progression. *Front Immunol*. 2021;12:658315.
41. Yuan J-L, Zheng W-X, Yan F, et al. Heme oxygenase-1 is a predictive biomarker for therapeutic targeting of advanced clear cell renal cell carcinoma treated with sorafenib or sunitinib. *Oncol Targets Ther*. 2015;8:2081.
42. Deng Y, Wu Y, Zhao P, et al. The Nrf2/HO-1 axis can be a prognostic factor in clear cell renal cell carcinoma. *Cancer Manag Res*. 2019;11:1221-1230.
43. Loboda A, Damulewicz M, Pyza E, Jozkowicz A, Dulak J. Role of Nrf2/HO-1 system in development, oxidative stress response and diseases: an evolutionarily conserved mechanism. *Cell Mol Life Sci*. 2016;73:3221-3247.
44. Chiang S-K, Chen S-E, Chang L-C. A dual role of heme oxygenase-1 in cancer cells. *Int J Mol Sci*. 2018;20:39.
45. Miyake M, Fujimoto K, Anai S, et al. Heme oxygenase-1 promotes angiogenesis in urothelial carcinoma of the urinary bladder. *Oncol Rep*. 2011;25:653-660.
46. Mendonsa AM, Na T-Y, Gumbiner BM. E-cadherin in contact inhibition and cancer. *Oncogene*. 2018;37:4769-4780.
47. Mikami S, Oya M, Mizuno R, Kosaka T, Katsube K-I, Okada Y. Invasion and metastasis of renal cell carcinoma. *Med Mol Morphol*. 2014;47:63-67.
48. Song Y, Washington MK, Crawford HC. Loss of FOXA1/2 is essential for the epithelial-to-mesenchymal transition in pancreatic cancer. *Cancer Res*. 2010;70:2115-2125.
49. Dohi Y, Ikura T, Hoshikawa Y, et al. Bach1 inhibits oxidative stress-induced cellular senescence by impeding p53 function on chromatin. *Nat Struct Mol Biol*. 2008;15:1246-1254.
50. Zhu G-D, Liu F, Ouyang S, et al. BACH1 promotes the progression of human colorectal cancer through BACH1/CXCR4 pathway. *Biochem Biophys Res Commun*. 2018;499:120-127.
51. Cohen B, Tempelhof H, Raz T, et al. BACH family members regulate angiogenesis and lymphangiogenesis by modulating VEGFC expression. *Life Sci Alliance*. 2020;3:e202000666.
52. Zhao D, Yang J, Yang L. Insights for oxidative stress and mTOR signaling in myocardial ischemia/reperfusion injury under diabetes. *Oxid Med Cell Longev*. 2017;2017:1-12.

SUPPORTING INFORMATION

Additional supporting information can be found online in the Supporting Information section at the end of this article.

How to cite this article: Takemoto K, Kobatake K, Miura K, et al. BACH1 promotes clear cell renal cell carcinoma progression by upregulating oxidative stress-related tumorigenicity. *Cancer Sci*. 2023;114:436-448. doi: [10.1111/cas.15607](https://doi.org/10.1111/cas.15607)